



EUROPEAN ORGANIZATION FOR NUCLEAR RESEARCH

CERN-PPE/93-68
April 26, 1993

Determination of the Effective Electroweak Mixing Angle from Z Decays

L3 Collaboration

Abstract

The effective electroweak mixing angle $\sin^2 \bar{\theta}_w$ is measured from the production and decay of the Z boson in e^+e^- interactions. The data sample corresponds to an integrated luminosity of 18 pb^{-1} with about 420,000 hadronic and 40,000 leptonic Z decays. The mixing angle $\sin^2 \bar{\theta}_w$ is determined from several independent measurements: the leptonic and hadronic cross sections, the forward-backward asymmetries of charged leptons and b-quarks, and the τ -polarization. The results are found to be in good agreement with each other. The value of $\sin^2 \bar{\theta}_w$ from a fit to the asymmetries in a model independent method is 0.2321 ± 0.0021 and from a global fit to the data in the Standard Model framework is 0.2328 ± 0.0013 .

(Submitted to *Physics Letters B*)

1 Introduction

In the Standard Model of electroweak interactions [1], the electroweak mixing angle, θ_w , describes the mixing of the gauge fields W_3 and B of the local gauge group $SU(2)_L \times U(1)$. For the calculation of electroweak processes between fermions, four basic input parameters are required apart from fermion masses and quark mixing angles. The on-shell renormalisation scheme uses α , M_W , M_Z and the mass of the Higgs particle as input parameters. QCD [2] adds one more parameter, the strong coupling constant α_s . The electroweak mixing angle is defined by the relation

$$\sin^2 \theta_w = 1 - \frac{M_W^2}{M_Z^2} \quad (1)$$

where M_W and M_Z are the physical masses of the W and Z boson.

The Z mass is measured from the peak position of the Z lineshape at LEP with high precision [3, 4]. α_s is determined at LEP from analysis of hadronic Z decays [5]. An additional constraint can be obtained from the Fermi coupling constant, G_F , measured in muon decay. As α is well determined, the Standard Model still requires two unknown parameters, typically taken as the mass of the top quark, M_t , and the mass of the Higgs particle, M_H . One can consider $\sin^2 \theta_w$ instead of M_t as a free parameter. The effect of the Higgs mass on cross sections and asymmetries is rather small. At LEP we measure the *effective* electroweak mixing angle, $\sin^2 \bar{\theta}_w$, which includes weak radiative corrections.

In this paper, we use the measurements of the cross sections of hadrons and charged leptons [3], the forward-backward asymmetries of the charged leptons (A_{FB}^{ℓ}) [3] and bottom quarks (A_{FB}^b) [6], and the τ -polarization asymmetry (P_{τ}) [7] for a precise determination of the electroweak mixing angle. We test if the Standard Model describes the different measurements with a unique value of the electroweak mixing angle.

2 Effective Coupling Constants

It is important to determine the electroweak parameters independently of assumptions about the two unknown parameters, M_t and M_H . The model independent approach introduces an additional parameter ρ which denotes the ratio of the neutral to charged current coupling constants. This ratio is unity in the Standard Model at the tree level. Radiative corrections can be separated into QED corrections and weak corrections. The QED corrections, which depend on the acceptance of the detector and on cuts used in the analysis, are always taken into account for calculating the theoretical predictions. Since the weak corrections cannot be calculated outside the framework of the Standard Model, we do not apply weak corrections, but absorb them into the definition of the fitted parameters. As a result, at LEP one measures the effective electroweak mixing angle, $\sin^2 \bar{\theta}_w^f$, where f denotes the flavour, which absorbs the weak corrections :

$$\sin^2 \bar{\theta}_w^f = k_f \sin^2 \theta_w, \quad (2)$$

k_f accounts for all weak corrections. Standard Model calculations show that k_f is flavour independent within 0.04% with the exception of b-quarks. We, therefore, take $\sin^2 \bar{\theta}_w$ to be the effective electroweak mixing angle for all fermions except b-quarks. For b-quarks the vertex

correction is large due to the virtual top quark contribution. The two determinations of $\sin^2 \bar{\theta}_w$ can be related by [8]:

$$\sin^2 \bar{\theta}_w^b = \left(1 + \frac{2}{3} \Delta \bar{\rho}\right) \sin^2 \bar{\theta}_w, \quad (3)$$

$$\Delta \bar{\rho} \simeq \frac{3G_F M_t^2}{8\pi^2 \sqrt{2}} \quad (4)$$

For $M_t = 150$ GeV the value of $\sin^2 \bar{\theta}_w^b$ is 0.4% larger than $\sin^2 \bar{\theta}_w$. The parameter $\bar{\rho} (\equiv 1 + \Delta \bar{\rho})$ is the effective ρ parameter.

The effective vector and axial-vector couplings of the Z to light fermion pairs are given by

$$\bar{g}_a = \sqrt{\bar{\rho}} I_3 \quad (5)$$

$$\bar{g}_v = \sqrt{\bar{\rho}} (I_3 - 2Q \sin^2 \bar{\theta}_w) \quad (6)$$

where I_3 and Q are respectively the weak isospin and charge of the fermion.

The expressions for A_{FB}^ℓ , A_{FB}^b and P_τ in terms of $\sin^2 \bar{\theta}_w$ at $\sqrt{s} = M_Z$ are [9]:

$$A_{\text{FB}}^\ell(M_Z^2) = \frac{3(1 - 4 \sin^2 \bar{\theta}_w)^2}{[1 + (1 - 4 \sin^2 \bar{\theta}_w)^2]^2 + \frac{K}{\bar{\rho}_\ell^2} \cdot \frac{\Gamma_Z^2}{M_Z^2}} \quad (7)$$

$$A_{\text{FB}}^b(M_Z^2) = \frac{3 \cdot (1 - 4 \sin^2 \bar{\theta}_w) \cdot \beta(1 - \frac{4}{3} \sin^2 \bar{\theta}_w^b)}{[1 + (1 - 4 \sin^2 \bar{\theta}_w)^2][\beta^2 + \frac{3-\beta^2}{2}(1 - \frac{4}{3} \sin^2 \bar{\theta}_w^b)^2] + \frac{K}{\bar{\rho}_\ell \bar{\rho}_b} \cdot \frac{\Gamma_Z^2}{M_Z^2} \frac{1}{9}(1 + 2 \frac{M_b^2}{M_Z^2})} \quad (8)$$

$$P_\tau(M_Z^2) = - \frac{2(1 - 4 \sin^2 \bar{\theta}_w) \cdot [1 + (1 - 4 \sin^2 \bar{\theta}_w)^2]}{[1 + (1 - 4 \sin^2 \bar{\theta}_w)^2]^2 + \frac{K}{\bar{\rho}_\ell^2} \cdot \frac{\Gamma_Z^2}{M_Z^2}} \quad (9)$$

where $\beta = \sqrt{1 - 4M_b^2/M_Z^2}$, M_b is the mass of the b-quark, $K = 16 \sin^4 \theta_w \cos^4 \theta_w$ and $\bar{\rho}_\ell$ and $\bar{\rho}_b$ are the $\bar{\rho}$ parameters for the leptons and b-quarks. In the above expressions, for the sake of clarity, the correction due to photon vacuum polarization has been omitted. For comparison with data we use the complete s -dependent expressions with QED corrections which take into account initial and final state radiation.

3 The L3 Detector

The fiducial solid angle of the L3 detector [10] is 99% of 4π . L3 consists of a time expansion chamber (TEC) for tracking charged particles, a high resolution electromagnetic calorimeter of BGO crystals, a barrel of scintillation counters, a hadron calorimeter with uranium absorber and proportional wire chamber readout and a muon spectrometer. The luminosity is determined from small-angle Bhabha scattering using BGO electromagnetic calorimetry in the polar angle ranges θ and $\pi - \theta$ between 24.93 and 69.94 mrad. All subdetectors are installed inside a 12 m diameter solenoidal magnet which provides a uniform 0.5 T field along the beam direction.

4 Event Selection

We briefly summarize the selection of various types of events; for details see ref [3, 6].

- The selection of $e^+e^- \rightarrow e^+e^-(\gamma)$ events is based mainly on information from the electromagnetic calorimeter. Background from hadronic events is suppressed by requiring that events have less than 8 reconstructed clusters in the electromagnetic calorimeter, and $\tau^+\tau^-$ events are rejected by requiring that the most energetic cluster in the electromagnetic calorimeter has energy $> 0.85 E_{\text{beam}}$.
- Events of type $e^+e^- \rightarrow \mu^+\mu^-(\gamma)$ are required to have two tracks in the muon chamber system with one muon track with momentum greater than $\frac{2}{3}E_{\text{beam}}$. Cosmic ray background is removed by demanding the muon track to be within 3 nsec of the beam gate.
- The selection of $e^+e^- \rightarrow \tau^+\tau^-(\gamma)$ events requires the total energy in the electromagnetic calorimeter to be larger than 2 GeV and the two most energetic electromagnetic clusters to have energies below 90% and 65% of the beam energy. This removes background from e^+e^- final states. Similarly the background from $\mu^+\mu^-$ is suppressed by requiring that the momentum measured in the muon chambers is less than $0.9 E_{\text{beam}}$ for the most energetic and $0.4 E_{\text{beam}}$ for the second most energetic muon candidate in the event. Hadronic events are suppressed by applying an upper limit of 12 calorimeter clusters.
- The event selection for $e^+e^- \rightarrow$ hadrons is based on the energy depositions in the electromagnetic and hadronic calorimeters. Backgrounds due to beam-wall interactions, beam-gas interactions, two-photon events and cosmic ray showers are suppressed by cuts on the total visible energy, E_{vis} , and by restricting the longitudinal and transverse energy imbalances to $|E_{\parallel}|/E_{\text{vis}} < 0.6$ and $|E_{\perp}|/E_{\text{vis}} < 0.5$.
- Hadronic events are used to further select $e^+e^- \rightarrow b\bar{b}$. We use electrons and muons from the semileptonic decay of b-quark to select these events. Because of the hard fragmentation and large mass of the b-quark, leptons from b-quark decay have large momentum (p) as well as large transverse momentum (p_{\perp}) with respect to the nearest jet. By putting a lower limit on both p (3-4 GeV) and p_{\perp} (1 GeV), $b\bar{b}$ event selection purity reaches 85%.

5 Results

This analysis is based on the following sets of data, summarized in Tables 1 to 3, corresponding to an integrated luminosity of $\simeq 18 \text{ pb}^{-1}$, collected with the L3 detector at LEP in 1990-91:

- 4 sets of cross section measurements of $e^+e^- \rightarrow e^+e^-$, $\mu^+\mu^-$, $\tau^+\tau^-$ and hadrons [5];
- 3 sets of forward-backward asymmetry measurements of charged leptons (A_{FB}^{ℓ}) in $e^+e^- \rightarrow e^+e^-$, $\mu^+\mu^-$ and $\tau^+\tau^-$ [5];
- Forward-backward asymmetry of b-quark in $e^+e^- \rightarrow b\bar{b}$ [6];
- Measurement of τ -polarization [7].

To fit the data, we use ZFITTER [11] in the L3 lineshape fitting program which uses MINUIT [12] for minimisation. ZFITTER takes into account initial and final state photon radiation and corrections due to photon vacuum polarization. Two separate fitting procedures are followed:

Standard Model fit: QED as well as weak radiative corrections are taken from the Standard Model. The free parameters are M_Z , top quark mass (M_t), Higgs boson mass (M_H) and the

Data 1990				
\sqrt{s} (GeV)	σ^{had} (nb)	σ^{ee} (nb)	$\sigma^{\mu\mu}$ (nb)	$\sigma^{\tau\tau}$ (nb)
88.231	4.53 ± 0.11	0.334 ± 0.030	0.268 ± 0.033	0.228 ± 0.037
89.236	8.50 ± 0.14	0.532 ± 0.034	0.387 ± 0.038	0.439 ± 0.047
90.238	18.60 ± 0.25	0.895 ± 0.050	0.929 ± 0.063	0.920 ± 0.077
91.230	30.38 ± 0.12	1.051 ± 0.019	1.476 ± 0.028	1.463 ± 0.033
92.226	21.78 ± 0.26	0.715 ± 0.043	1.115 ± 0.066	1.095 ± 0.078
93.228	12.36 ± 0.16	0.405 ± 0.029	0.505 ± 0.040	0.599 ± 0.051
94.223	8.20 ± 0.14	0.223 ± 0.022	0.404 ± 0.036	0.427 ± 0.043
sys. error	0.3%	0.5%	0.8%	1.5%

Data 1991				
\sqrt{s} (GeV)	σ^{had} (nb)	σ^{ee} (nb)	$\sigma^{\mu\mu}$ (nb)	$\sigma^{\tau\tau}$ (nb)
91.254	30.43 ± 0.10	1.030 ± 0.014	1.497 ± 0.020	1.505 ± 0.025
88.480	5.17 ± 0.09	0.400 ± 0.023	0.235 ± 0.021	0.236 ± 0.024
89.470	10.08 ± 0.12	0.574 ± 0.026	0.478 ± 0.028	0.531 ± 0.035
90.228	18.12 ± 0.18	0.792 ± 0.032	0.866 ± 0.039	0.885 ± 0.047
91.222	30.26 ± 0.13	1.065 ± 0.019	1.381 ± 0.026	1.447 ± 0.032
91.967	24.51 ± 0.24	0.798 ± 0.033	1.165 ± 0.048	1.224 ± 0.059
92.966	14.36 ± 0.16	0.431 ± 0.024	0.686 ± 0.036	0.641 ± 0.041
93.716	10.02 ± 0.13	0.302 ± 0.019	0.478 ± 0.028	0.535 ± 0.036
sys. error	0.2%	0.5%	0.5%	0.7%

Table 1: Measured hadronic and leptonic cross sections, extrapolated to the full solid angle (except σ^{ee}). σ^{ee} is the electron cross section measured in the range $44^\circ \leq \theta \leq 136^\circ$ with an acollinearity cut of $\zeta < 25^\circ$. An overall luminosity error of 0.6% has to be added to the systematic errors.

Data 1990			
\sqrt{s} (GeV)	A_{FB}^e	A_{FB}^μ	A_{FB}^τ
88.231	-0.034 ± 0.276	-0.39 ± 0.12	-0.42 ± 0.20
89.236	-0.205 ± 0.161	-0.04 ± 0.11	-0.09 ± 0.15
90.238	-0.111 ± 0.107	-0.184 ± 0.074	-0.18 ± 0.11
91.230	-0.023 ± 0.028	0.006 ± 0.021	0.07 ± 0.03
92.226	-0.042 ± 0.085	0.110 ± 0.066	-0.04 ± 0.10
93.228	0.053 ± 0.094	0.095 ± 0.091	0.11 ± 0.12
94.223	0.129 ± 0.148	0.134 ± 0.099	0.02 ± 0.13
sys. error	0.005	0.005	0.01
Data 1991			
\sqrt{s} (GeV)	A_{FB}^e	A_{FB}^μ	A_{FB}^τ
91.254	0.001 ± 0.020	0.018 ± 0.015	0.037 ± 0.021
88.480	-0.013 ± 0.157	-0.15 ± 0.10	-0.11 ± 0.13
89.470	-0.126 ± 0.099	-0.20 ± 0.07	-0.152 ± 0.083
90.228	-0.100 ± 0.075	-0.041 ± 0.052	-0.137 ± 0.070
91.222	0.019 ± 0.027	0.013 ± 0.021	-0.032 ± 0.029
91.967	0.103 ± 0.055	0.060 ± 0.045	0.042 ± 0.063
92.966	0.098 ± 0.072	0.122 ± 0.058	0.161 ± 0.079
93.716	0.165 ± 0.085	0.084 ± 0.067	0.058 ± 0.082
sys. error	0.005	0.005	0.006

Table 2: Measured forward-backward asymmetries of leptonic Z decays. A_{FB}^e is the s -channel contribution to the electron forward-backward asymmetry, extrapolated to the full solid angle. A_{FB}^μ and A_{FB}^τ are the asymmetries measured with an acollinearity cut of $\zeta < 15^\circ$.

\sqrt{s} (GeV)	A_{FB}^b
89.67	0.025 ± 0.051
91.24	0.097 ± 0.017
92.81	0.062 ± 0.042
\sqrt{s} (GeV)	P_τ
91.212	$-0.132 \pm 0.026 \pm 0.021$

Table 3: Forward-backward asymmetries of $b\bar{b}$ and τ polarization

strong coupling constant (α_s). In this fit ZFITTER accounts for contributions upto $\mathcal{O}(\alpha\alpha_s)$ and $\mathcal{O}(M_t^4)$.

Model Independent Method: QED corrections are taken into account with an energy dependent Breit-Wigner shape for the determination of Z parameters. A slight dependence on the Standard Model parameters M_t and M_H enters into this method for the calculation of the γ -Z interference term, and the t -channel and s - t interference terms in $e^+e^- \rightarrow e^+e^-$. The effect of this is studied by changing M_t in the range 90 to 250 GeV and M_H from 60 to 1000 GeV. The fitted value of M_Z changes by ${}^{+0.5}_{-1.0}$ MeV; the change in other parameters is found to be less than 5% of their error.

We have used the model independent method to determine the mass, the total width and partial widths by fitting the total cross sections for $e^+e^- \rightarrow e^+e^-$, $\mu^+\mu^-$, $\tau^+\tau^-$ and hadrons. In addition to the experimental errors, which include statistical and systematic uncertainties, we have taken into account the errors on the center of mass energy as estimated by the LEP energy working group [13]. The fitted values of the Z mass, total width and partial widths thus obtained are, with $\chi^2/\text{DOF} = 53/56$:

$$\begin{aligned} M_Z &= 91195 \pm 9 \text{ MeV} \\ \Gamma_Z &= 2490 \pm 11 \text{ MeV} \\ \Gamma_h &= 1747 \pm 11 \text{ MeV} \\ \Gamma_\ell &= 83.1 \pm 0.5 \text{ MeV} \end{aligned}$$

5.1 $\sin^2 \bar{\theta}_w$ in the Standard Model Framework

In this section we describe the determination of $\sin^2 \bar{\theta}_w$ in the Standard Model framework. Fits are carried out using ZFITTER with M_Z and M_t as the free parameters. $\sin^2 \bar{\theta}_w$ is then determined using the Standard Model relation. The data are fitted with a fixed value of $M_H = 300$ GeV and constraining the value of α_s to 0.124 ± 0.006 [5]. The effect of M_H is studied by varying it from 60 GeV to 1000 GeV. This effect is found to be ± 0.0001 in $\sin^2 \bar{\theta}_w$. The results from the following fits are summarized in Table 4.

$\sin^2 \bar{\theta}_w$ from Γ_ℓ : Here we fit to the measured value of Γ_ℓ obtained from the model independent fit to the cross section data. In addition we constrain M_Z to the measured value.

$\sin^2 \bar{\theta}_w$ from Γ_Z : The fit is carried out using the measured value of Γ_Z and M_Z from the cross section data.

$\sin^2 \bar{\theta}_w$ from A_{FB} : In these fits we use (i) the asymmetry data from charged leptons, (ii) A_{FB}^b , (iii) P_τ and (iv) all the asymmetry data : A_{FB}^ℓ , A_{FB}^b and P_τ . M_Z is constrained to the measured value given above.

$\sin^2 \bar{\theta}_w$ from cross section and asymmetry measurements : Here we perform a global fit to all the data, that is, the cross section data, the charged lepton asymmetries, the $b\bar{b}$ asymmetry and the τ -polarization, in the framework of the Standard Model. A good fit is obtained with $\chi^2/\text{DOF} = 84/105$.

The values of $\sin^2 \bar{\theta}_w$ and M_t determined with the global fit in the Standard Model framework are :

$$\begin{aligned} \sin^2 \bar{\theta}_w &= 0.2328 \pm 0.0013 \pm 0.0001 \\ M_t &= 152^{+36}_{-46} \pm 20 \text{ GeV} \end{aligned}$$

corresponding to a value of $\sin^2 \theta_w$, as defined in eq. (1), to be $0.2268^{+0.0050}_{-0.0045} {}^{+0.0003}_{-0.0005}$. The second error corresponds to a variation of the Higgs mass between 60 and 1000 GeV. Figure 1 shows contour plots of $\sin^2 \bar{\theta}_w$ vs M_Z , and $\sin^2 \bar{\theta}_w$ vs M_t at the 68% CL for different values of M_H .

Measurements Used	$\sin^2 \bar{\theta}_w$
M_Z, Γ_ℓ	$0.2351 \pm_{0.0019}^{0.0009} *$
M_Z, Γ_Z	0.2330 ± 0.0017
M_Z, A_{FB}^ℓ	$0.2279 \pm_{0.0035}^{0.0040}$
M_Z, A_{FB}^b	$0.2335 \pm_{0.0030}^{0.0025} *$
M_Z, P_τ	$0.2326 \pm_{0.0044}^{0.0034} *$
$M_Z, A_{\text{FB}}^\ell, A_{\text{FB}}^b, P_\tau$	0.2319 ± 0.0022
All data	0.2328 ± 0.0013

Table 4: $\sin^2 \bar{\theta}_w$ determined in the Standard Model framework. In the determinations using M_Z and only Γ_ℓ , A_{FB}^b and P_τ , the positive errors quoted, denoted by “*”, are constrained by the measurements of α , G_F , M_Z which restrict $\sin^2 \bar{\theta}_w \leq 0.2360$ at $M_H = 300$ GeV.

5.2 $\sin^2 \bar{\theta}_w$ in the Model Independent Method

In this section we describe the model independent determination of $\sin^2 \bar{\theta}_w$ using all the asymmetry data and the four cross section data sets. The cross sections determine the mass and total width of Z, while the asymmetries measure $\sin^2 \bar{\theta}_w$. The dependence of the asymmetries on $\sin^2 \bar{\theta}_w$ are described by eqs.(7-9); they depend weakly on M_Z and Γ_Z . Fits have been carried out using ZFITTER in the model independent method ¹⁾. Lepton universality is assumed in carrying out the fits. The results are summarized in Table 5.

$\sin^2 \bar{\theta}_w$ from A_{FB}^ℓ : Here we use the 3 sets of forward-backward asymmetry measurements (A_{FB}^ℓ) along with the four sets of cross section data. Free parameters of the fit are: $M_Z, \Gamma_Z, \Gamma_h, \bar{\rho}$ and $\sin^2 \bar{\theta}_w$.

$\sin^2 \bar{\theta}_w$ from A_{FB}^b : In this fit we use the $b\bar{b}$ asymmetry measurements together with the cross section data. Compared to the A_{FB}^ℓ case, we need $\sin^2 \bar{\theta}_w^b$ and $\bar{\rho}_b$ for A_{FB}^b as in eq.(8). We rewrite $\sin^2 \bar{\theta}_w^b$ in terms of $\sin^2 \bar{\theta}_w$ and M_t using eq.(3) and take $\bar{\rho}_b$ from the Standard Model. Thus our free parameters of the fit are the same as above. The effect of M_t on the fitted $\sin^2 \bar{\theta}_w$ is studied by varying it from 90 to 250 GeV, and it is found to change the fitted value by less than 0.0001. We have also studied the effect of M_t arising from eq.(3) by refitting the data for a fixed value of $\bar{\rho}_b$. We find that the variation in M_t from

¹⁾We have repeated the fits by using only the asymmetry data and by constraining M_Z and Γ_Z to our measured values. In this procedure, one needs to assume $\bar{\rho}$ from the Standard Model. The values of $\sin^2 \bar{\theta}_w$ thus obtained are found to differ from the values quoted in Table 5 by less than 0.0001. The effect of taking $\bar{\rho}$ from the Standard Model is studied by changing M_t from 90 to 250 GeV, and it is found to change the fitted value of $\sin^2 \bar{\theta}_w$ by less than 0.00002.

0 to 250 GeV changes $\sin^2 \bar{\theta}_w$ by only 0.00004. Thus at current precision we can replace $\sin^2 \bar{\theta}_w^b$ by $\sin^2 \bar{\theta}_w$ in eq.(8) [14].

$\sin^2 \bar{\theta}_w$ from P_τ : The free parameters in this case are identical to the first case.

$\sin^2 \bar{\theta}_w$ from $A_{\text{FB}}^\ell, A_{\text{FB}}^b, P_\tau$: The fitted values of $\sin^2 \bar{\theta}_w$, as measured in the above three cases, refer to the same definition of $\sin^2 \bar{\theta}_w$ [15]. Hence to get the best value of $\sin^2 \bar{\theta}_w$ from our asymmetry measurements we carry out a simultaneous fit to all the three types of the asymmetry data along with the cross section data assuming lepton universality.

The combined fit to all data in the model independent method yields :

$$\begin{aligned}\sin^2 \bar{\theta}_w &= 0.2321 \pm 0.0021 \\ \bar{\rho} &= 0.9957 \pm 0.0060\end{aligned}$$

Figure 2 shows the 68% and 95% confidence level contour plots of $\sin^2 \bar{\theta}_w$ vs $\bar{\rho}$ together with Standard Model predictions.

Measurements Used	χ^2/DOF	$\sin^2 \bar{\theta}_w$	$\bar{\rho}$
σ 's, A_{FB}^ℓ	82/100	0.2283 ± 0.0036	0.9933 ± 0.0063
σ 's, A_{FB}^b	55/58	0.2336 ± 0.0029	0.9961 ± 0.0063
σ 's, P_τ	53/56	0.2326 ± 0.0043	0.9956 ± 0.0065
σ 's, $A_{\text{FB}}^\ell, A_{\text{FB}}^b, P_\tau$	86/104	0.2321 ± 0.0021	0.9957 ± 0.0060

Table 5: $\sin^2 \bar{\theta}_w$ determined in the model independent method

6 Conclusions

From a data sample of 420,000 hadronic and 40,000 leptonic Z decays recorded by the L3 detector we have determined the effective electroweak mixing angle, $\sin^2 \bar{\theta}_w$, with several methods: (i) from Standard Model fits to M_Z and Γ_ℓ , M_Z and Γ_Z , M_Z and A_{FB} 's, (ii) from a global fit to the cross section and asymmetry data in the Standard Model framework and (iii) from A_{FB}^ℓ , A_{FB}^b and P_τ in a model independent way. The results, as summarized in Figure 3, are in very good agreement with each other.

The model independent value of $\sin^2 \bar{\theta}_w$ from the three measured asymmetries is: 0.2321 ± 0.0021 . Within the framework of the Standard Model a global fit to all the data yields $\sin^2 \bar{\theta}_w = 0.2328 \pm 0.0013$.

Acknowledgement

We wish to express our gratitude to the CERN accelerator divisions for the excellent performance of the LEP machine. We acknowledge the efforts of all engineers and technicians who have participated in the construction and maintenance of this experiment.

The L3 Collaboration:

O. Adriani,¹⁴ M. Aguilar-Benitez,²³ S. Ahlen,⁹ J. Alcaraz,¹⁵ A. Aloisio,²⁶ G. Alverson,¹⁰ M. G. Alviggi,²⁶ G. Ambrosi,³¹ Q. An,¹⁶ H. Anderhub,⁴⁵ A. L. Anderson,¹³ V. P. Andreev,³⁵ L. Antonov,³⁹ D. Antreasyan,⁷ P. Arce,²³ A. Arefiev,²⁵ A. Atamanchuk,³⁵ T. Azemoon,³ T. Aziz,^{1,8} P. V. K. S. Baba,¹⁶ P. Bagnaia,³⁴ J. A. Bakken,³³ L. Baksay,⁴¹ R. C. Ball,³ S. Banerjee,⁶ J. Bao,⁵ R. Barillere,¹⁵ L. Barone,³⁴ A. Baschirotto,²⁴ R. Battiston,³¹ A. Bay,¹⁷ F. Becattini,¹⁴ J. Bechtluft,¹ R. Becker,¹ U. Becker,^{13,45} F. Behner,⁴⁵ J. Behrens,⁴⁵ Gy. L. Bencze,¹¹ J. Berdugo,²³ P. Berges,¹³ B. Bertucci,³¹ B. L. Betev,^{39,45} M. Biasini,³¹ A. Biland,⁴⁵ G. M. Bilei,³¹ R. Bizzarri,³⁴ J. J. Blaising,⁴ G. J. Bobbink,^{15,2} R. Bock,¹ A. Böhm,¹ B. Borgia,³⁴ M. Bosetti,²⁴ D. Bourilkov,²⁸ M. Bourquin,¹⁷ D. Boutigny,⁴ B. Bouwens,² E. Brambilla,²⁶ J. G. Branson,³⁶ I. C. Brock,³² M. Brooks,²¹ A. Bujak,⁴² J. D. Burger,¹³ W. J. Burger,¹⁷ J. Busenitz,⁴¹ A. Buytenhuijs,²⁸ X. D. Cai,¹⁶ M. K. Capell,¹³ M. Caria,³¹ G. Carlino,²⁶ A. M. Cartacci,⁴ R. Castello,²⁴ M. Cerrada,²³ F. Cesaroni,³⁴ Y. H. Chang,¹³ U. K. Chaturvedi,¹⁶ M. Chemarin,²² A. Chen,⁴⁷ C. Chen,⁶ G. M. Chen,⁶ H. F. Chen,¹⁸ H. S. Chen,⁶ M. Chen,¹³ W. Y. Chen,⁴⁷ G. Chiefari,²⁶ C. Y. Chien,⁵ M. T. Choi,⁴⁰ S. Chung,¹³ C. Cividini,¹⁴ I. Clare,¹³ R. Clare,¹³ T. E. Coan,²¹ H. O. Cohn,²⁹ G. Coignet,⁴ N. Colino,¹⁵ A. Contin,⁷ X. T. Cui,¹⁶ X. Y. Cui,¹⁶ T. S. Dai,¹³ R. D' Alessandro,¹⁴ R. de Asmundis,²⁶ A. Degré,⁴ K. Deiters,⁴³ E. Dénes,¹¹ P. Denes,³³ F. DeNotaristefani,³⁴ M. Dhina,⁴⁵ D. DiBitonto,⁴¹ M. Diemoz,³⁴ H. R. Dimitrov,³⁹ C. Dionisi,^{34,15} L. Djambazov,⁴⁵ M. T. Dova,¹⁶ E. Drago,²⁶ D. Duchesneau,¹⁷ P. Duinker,² I. Duran,³⁷ S. Easo,³¹ H. El Mamouni,²² A. Engler,³² F. J. Eppling,¹³ F. C. Erné,² P. Extermann,¹⁷ R. Fabbretti,⁴³ M. Fabre,⁴³ S. Falciano,³⁴ S. J. Fan,³⁶ O. Fackler,²⁰ J. Fay,²² M. Felcini,¹⁵ T. Ferguson,³² D. Fernandez,²³ G. Fernandez,²³ F. Ferroni,³⁴ H. Fesefeldt,¹ E. Fiandrini,³¹ J. Field,¹⁷ F. Filthaut,²⁸ G. Finocchiaro,³⁴ P. H. Fisher,⁵ G. Forconi,¹⁷ T. Foreman,² L. Fredj,¹⁷ K. Freudenreich,⁴⁵ W. Friebel,⁴⁴ M. Fukushima,¹³ M. Gailloud,¹⁹ Yu. Galaktionov,^{25,13} E. Gallo,¹⁴ S. N. Ganguli,^{15,8} P. Garcia-Abia,²³ D. Gele,²² S. Gentile,^{34,15} S. Goldfarb,¹⁰ Z. F. Gong,¹⁸ E. Gonzalez,²³ A. Gougas,⁵ D. Goujon,¹⁷ G. Gratta,³⁰ M. Gruenewald,¹⁵ C. Gu,¹⁶ M. Guanziroli,¹⁶ J. K. Guo,³⁸ V. K. Gupta,³³ A. Gurtu,⁸ H. R. Gustafson,³ L. J. Gutay,⁴² K. Hangarter,¹ B. Hartmann,¹ A. Hasan,¹⁶ D. Hauschildt,² C. F. He,³⁸ J. T. He,⁶ T. Hebbeker,¹⁵ M. Hebert,³⁶ G. Herten,¹³ A. Hervé,¹⁵ K. Hilgers,¹ H. Hofer,⁴⁵ H. Hoorani,¹⁷ G. Hu,¹⁶ G. Q. Hu,³⁸ B. Ille,²² M. M. Ilyas,¹⁶ V. Innocente,¹⁵ H. Janssen,¹⁵ S. Jezequel,⁴ B. N. Jin,⁶ L. W. Jones,³ A. Kasser,¹⁹ R. A. Khan,¹⁶ Yu. Kamyshev,²⁹ P. Kapinos,^{35,44} J. S. Kapustinsky,²¹ Y. Karyotakis,¹⁵ M. Kaur,¹⁶ S. Khokhar,¹⁶ M. N. Kienzle-Focacci,¹⁷ J. K. Kim,⁴⁰ S. C. Kim,⁴⁰ Y. G. Kim,⁴⁰ W. W. Kinnison,²¹ A. Kirkby,³⁰ D. Kirkby,³⁰ S. Kirsch,⁴⁴ W. Kittel,²⁸ A. Klimentov,^{13,25} R. Klöckner,¹ A. C. König,²⁸ E. Koffeman,² O. Kornadt,¹ V. Koutsenko,^{13,25} A. Koulbardis,³⁵ R. W. Kraemer,³² T. Kramer,¹³ V. R. Krastev,^{39,31} W. Krenz,¹ A. Krivshich,³⁵ H. Kuijten,²⁸ K. S. Kumar,¹² A. Kunin,^{13,25} G. Landi,⁴ D. Lanske,¹ S. Lanzano,²⁶ A. Lebedev,¹³ P. Lebrun,²² P. Lecomte,⁴⁵ P. Lecoq,¹⁵ P. Le Coultre,⁴⁵ D. M. Lee,²¹ I. Leedom,¹⁰ C. Leggett,³ J. M. Le Goff,¹⁵ R. Leiste,⁴⁴ M. Lenti,⁴ E. Leonardi,³⁴ X. Leytens,² C. Li,^{18,16} H. T. Li,⁶ P. J. Li,³⁸ J. Y. Liao,³⁸ W. T. Lin,⁴⁷ Z. Y. Lin,¹⁸ F. L. Linde,¹⁵ B. Lindemann,¹ L. Lista,²⁶ Y. Liu,¹⁶ W. Lohmann,^{44,15} E. Longo,³⁴ Y. S. Lu,⁶ J. M. Lubbers,¹⁵ K. Lübelmeyer,¹ C. Luci,³⁴ D. Luckey,^{7,13} L. Ludovici,³⁴ L. Luminari,³⁴ W. Lustermaan,⁴⁴ J. M. Ma,⁶ W. G. Ma,¹⁸ M. MacDermott,⁴⁵ P. K. Malhotra,^{9,†} R. Malik,¹⁶ A. Malinin,²⁵ C. Mañá,²³ M. Maolinbay,⁴⁵ P. Marchesini,⁴⁵ F. Marion,⁴ A. Marin,⁹ J. P. Martin,²² L. Martinez-Laso,²³ F. Marzano,³⁴ G. G. G. Massaro,² K. Mazumdar,¹⁷ P. McBride,¹² T. McMahon,⁴² D. McNally,⁴⁵ M. Merk,³² L. Merola,²⁶ M. Meschini,¹⁴ W. J. Metzger,²⁸ Y. Mi,¹⁹ G. B. Mills,²¹ Y. Mir,¹⁶ G. Mirabelli,³⁴ J. Mnich,¹ M. Möller,¹ B. Monteleoni,¹⁴ R. Morand,⁴ S. Morganti,³⁴ N. E. Moulai,¹⁶ R. Mouton,³⁰ S. Müller,¹ A. Nadtochy,³⁵ E. Nagy,¹¹ M. Napolitano,²⁶ F. Nessi-Tedaldi,⁴⁵ H. Newman,³⁰ C. Neyer,⁴⁵ M. A. Niaz,¹⁶ A. Nippe,¹ H. Nowak,⁴⁴ G. Organtini,³⁴ D. Pandoulas,¹ S. Paoletti,¹⁴ P. Paolucci,²⁶ G. Pascala,³⁴ G. Passaleva,^{14,31} S. Patricelli,²⁶ T. Paul,⁵ M. Pauluzzi,³¹ C. Paus,¹ F. Pauss,⁴⁵ Y. J. Pei,¹ S. Pensotti,²⁴ D. Perret-Gallix,⁴ J. Perrier,¹⁷ A. Pevsner,⁵ D. Piccolo,²⁶ M. Pieri,¹⁵ P. A. Piroué,³³ F. Plasil,²⁹ V. Plyaskin,²⁵ M. Pohl,⁴⁵ V. Pojidaev,^{25,14} H. Postema,¹³ Z. D. Qi,³⁸ J. M. Qian,³ K. N. Qureshi,¹⁶ R. Raghavan,⁸ G. Rahal-Callot,⁴⁵ P. G. Rancoita,²⁴ M. Rattaggi,²⁴ G. Raven,² P. Razis,²⁷ K. Read,²⁹ D. Ren,⁴⁵ Z. Ren,¹⁶ M. Rescigno,³⁴ S. Reucroft,¹⁰ A. Ricker,¹ S. Riemann,⁴⁴ B. C. Riemers,⁴² K. Riles,³ O. Rind,³ H. A. Rizvi,¹⁶ F. J. Rodriguez,²³ B. P. Roe,³ M. Röhner,¹ L. Romero,²³ S. Rosier-Lees,⁴ R. Rosmalen,²⁶ Ph. Rossetti,¹⁹ W. van Rossum,² S. Roth,¹ A. Rubbia,¹³ J. A. Rubio,¹⁵ H. Rykaczewski,⁴⁵ M. Sachwitz,⁴⁴ J. Salicio,¹⁵ J. M. Salicio,²³ G. S. Sanders,²¹ A. Santocchia,³¹ M. S. Sarakinos,¹³ G. Sartorelli,^{7,16} M. Sassowsky,¹ G. Sauvage,⁴ V. Schegelsky,³⁵ D. Schmitz,¹ P. Schmitz,¹ M. Schneegans,⁴ H. Schopper,⁴⁶ D. J. Schotanus,²⁸ S. Shotkin,¹³ H. J. Schreiber,⁴⁴ J. Shukla,³² R. Schulte,¹ S. Schulte,¹ K. Schultze,¹ J. Schwenke,¹ G. Schwering,¹ C. Sciacca,²⁶ I. Scott,¹² R. Sehgal,¹⁶ P. G. Seiler,⁴³ J. C. Sens,^{15,2} L. Servoli,³¹ I. Sheer,³⁶ D. Z. Shen,³⁶ S. Shevchenko,³⁰ X. R. Shi,³⁰ E. Shumilov,²⁵ V. Shoutko,²⁵ D. Son,⁴⁰ A. Sopczak,³⁶ C. Spartiotis,⁵ T. Spickermann,¹ P. Spillantini,¹⁴ R. Starosta,¹ M. Steuer,^{7,13} D. P. Stickland,³³ F. Sticozzi,¹³ H. Stone,¹² K. Strauch,¹² B. C. Stringfellow,⁴² K. Sudhakar,⁸ G. Sultanov,¹⁶ L. Z. Sun,^{18,16} G. F. Susinno,¹⁷ H. Suter,⁴⁵ J. D. Swain,¹⁶ A. A. Syed,²⁸ X. W. Tang,⁶ L. Taylor,¹⁰ G. Terzi,²⁴ Samuel C. C. Ting,¹³ S. M. Ting,¹³ M. Tonutti,¹ S. C. Tonwar,⁸ J. Tóth,¹¹ A. Tsaregorodtsev,³⁵ G. Tsipolitis,³² C. Tully,³³ K. L. Tung,⁶ J. Ulbricht,⁴⁵ L. Urbán,¹¹ U. Uwer,¹ E. Valente,³⁴ R. T. Van de Walle,²⁸ I. Vetlitsky,²⁵ G. Viertel,⁴⁵ P. Vikas,¹⁶ U. Vikas,¹⁶ M. Vivargent,⁴ H. Vogel,³² H. Vogt,⁴⁴ I. Vorobiev,²⁵ A. A. Vorobyov,³⁵ L. Vuilleumier,¹⁹ M. Wadhwa,⁴ W. Wallraff,¹ C. Wang,¹³ C. R. Wang,¹⁸ G. H. Wang,³² X. L. Wang,¹⁸ Y. F. Wang,¹³ Z. M. Wang,^{16,18} C. Warner,¹ A. Weber,¹ J. Weber,⁴⁵ R. Weill,¹⁹ T. J. Wenaus,²⁰ J. Wenninger,¹⁷ M. White,¹³ C. Willmott,²³ F. Wittgenstein,¹⁵ D. Wright,³³ S. X. Wu,¹⁶ S. Wynhoff,¹ B. Wyslouch,¹³ Y. Y. Xie,³⁸ J. G. Xu,⁶ Z. Z. Xu,¹⁸ Z. L. Xue,³⁸ D. S. Yan,³⁸ B. Z. Yang,¹⁸ C. G. Yang,⁶ G. Yang,¹⁶ C. H. Ye,¹⁶ J. B. Ye,¹⁸ Q. Ye,¹⁶ S. C. Yeh,⁴⁷ Z. W. Yin,³⁸ J. M. You,¹⁶ N. Yunus,¹⁶ M. Yzerman,² C. Zaccardelli,³⁰ P. Zemp,⁴⁵ M. Zeng,¹⁶ Y. Zeng,¹ D. H. Zhang,² Z. P. Zhang,^{18,16} B. Zhou,⁹ G. J. Zhou,⁶ J. F. Zhou,¹ R. Y. Zhu,³⁰ A. Zichichi,^{7,15,16} B. C. C. van der Zwaan,²

-
- 1 I. Physikalisches Institut, RWTH, W-5100 Aachen, FRG[§]
 - III. Physikalisches Institut, RWTH, W-5100 Aachen, FRG[§]
 - 2 National Institute for High Energy Physics, NIKHEF, NL-1009 DB Amsterdam, The Netherlands
 - 3 University of Michigan, Ann Arbor, MI 48109, USA
 - 4 Laboratoire d'Annecy-le-Vieux de Physique des Particules, LAPP, IN2P3-CNRS, BP 110, F-74941 Annecy-le-Vieux CEDEX, France
 - 5 Johns Hopkins University, Baltimore, MD 21218, USA
 - 6 Institute of High Energy Physics, IHEP, 100039 Beijing, China
 - 7 INFN-Sezione di Bologna, I-40126 Bologna, Italy
 - 8 Tata Institute of Fundamental Research, Bombay 400 005, India
 - 9 Boston University, Boston, MA 02215, USA
 - 10 Northeastern University, Boston, MA 02115, USA
 - 11 Central Research Institute for Physics of the Hungarian Academy of Sciences, H-1525 Budapest 114, Hungary[†]
 - 12 Harvard University, Cambridge, MA 02139, USA
 - 13 Massachusetts Institute of Technology, Cambridge, MA 02139, USA
 - 14 INFN Sezione di Firenze and University of Florence, I-50125 Florence, Italy
 - 15 European Laboratory for Particle Physics, CERN, CH-1211 Geneva 23, Switzerland
 - 16 World Laboratory, FBLJA Project, CH-1211 Geneva 23, Switzerland
 - 17 University of Geneva, CH-1211 Geneva 4, Switzerland
 - 18 Chinese University of Science and Technology, USTC, Hefei, Anhui 230 029, China
 - 19 University of Lausanne, CH-1015 Lausanne, Switzerland
 - 20 Lawrence Livermore National Laboratory, Livermore, CA 94550, USA
 - 21 Los Alamos National Laboratory, Los Alamos, NM 87544, USA
 - 22 Institut de Physique Nucléaire de Lyon, IN2P3-CNRS, Université Claude Bernard, F-69622 Villeurbanne Cedex, France
 - 23 Centro de Investigaciones Energeticas, Medioambientales y Tecnológicas, CIEMAT, E-28040 Madrid, Spain
 - 24 INFN-Sezione di Milano, I-20133 Milan, Italy
 - 25 Institute of Theoretical and Experimental Physics, ITEP, Moscow, Russia
 - 26 INFN-Sezione di Napoli and University of Naples, I-80125 Naples, Italy
 - 27 Department of Natural Sciences, University of Cyprus, Nicosia, Cyprus
 - 28 University of Nymegen and NIKHEF, NL-6525 ED Nymegen, The Netherlands
 - 29 Oak Ridge National Laboratory, Oak Ridge, TN 37831, USA
 - 30 California Institute of Technology, Pasadena, CA 91125, USA
 - 31 INFN-Sezione di Perugia and Università Degli Studi di Perugia, I-06100 Perugia, Italy
 - 32 Carnegie Mellon University, Pittsburgh, PA 15213, USA
 - 33 Princeton University, Princeton, NJ 08544, USA
 - 34 INFN-Sezione di Roma and University of Rome, "La Sapienza", I-00185 Rome, Italy
 - 35 Nuclear Physics Institute, St. Petersburg, Russia
 - 36 University of California, San Diego, CA 92093, USA
 - 37 Dept. de Fisica de Particulas Elementales, Univ. de Santiago, E-15706 Santiago de Compostela, Spain
 - 38 Shanghai Institute of Ceramics, SIC, Shanghai, China
 - 39 Bulgarian Academy of Sciences, Institute of Mechatronics, BU-1113 Sofia, Bulgaria
 - 40 Center for High Energy Physics, Korea Advanced Inst. of Sciences and Technology, 305-701 Taejon, Republic of Korea
 - 41 University of Alabama, Tuscaloosa, AL 35486, USA
 - 42 Purdue University, West Lafayette, IN 47907, USA
 - 43 Paul Scherrer Institut, PSI, CH-5232 Villigen, Switzerland
 - 44 DESY-Institut für Hochenergiephysik, O-1615 Zeuthen, FRG
 - 45 Eidgenössische Technische Hochschule, ETH Zürich, CH-8093 Zürich, Switzerland
 - 46 University of Hamburg, W-2000 Hamburg, FRG
 - 47 High Energy Physics Group, Taiwan, China
- § Supported by the German Bundesministerium für Forschung und Technologie
† Supported by the Hungarian OTKA fund under contract number 2970.
‡ Deceased.

References

- [1] S.L. Glashow, Nucl. Phys. **22** (1961) 579;
S. Weinberg, Phys. Rev. Lett. **19** (1967) 1264;
A. Salam, "Elementary Particle Theory", Ed: N. Svartholm, Stockholm, "Almqvist and Wiksell" (1968), 367.
- [2] M. Gell-Mann, Acta Phys. Austriaca Suppl. **IX** (1972) 733;
H. Fritzsche and M. Gell-Mann, 16th International Conference on High Energy Physics, Batavia, 1972; editors J.D. Jackson and A. Roberts, National Accelerator Laboratory (1972);
H. Fritzsche, M. Gell-Mann and H. Leytwyler, Phys. Lett. **B 47** (1973) 365;
D.J. Gross and F. Wilczek, Phys. Rev. Lett. **30** (1973) 1343;
D.J. Gross and F. Wilczek, Phys. Rev. **D 8** (1973) 3633;
H.D. Politzer, Phys. Rev. Lett. **30** (1973) 1346;
G. 't Hooft, Nucl. Phys. **B 33** (1971) 173.
- [3] L3 Collaboration, B.Adeva *et al.*: Z.Phys. **C51** (1991) 179.
- [4] ALEPH Collaboration, D.Decamp *et al.*: Z. Phys. **C53** (1992) 1;
DELPHI Collaboration, P.Abreu *et al.*: Nucl. Phys. **B367** (1991) 3;
OPAL Collaboration, G.Alexander *et al.*: Z. Phys. **C52** (1991) 175;
The LEP Collaboration, ALEPH, DELPHI, L3, OPAL: Phys. Lett. **B276** (1992) 247;
The Working Group on LEP Energy and the LEP Collaborations, ALEPH, DELPHI, L3 and OPAL: CERN-PPE/93-53, March 1993.
- [5] L3 Collaboration, O.Adriani *et al.*: CERN preprint, CERN-PPE/93-31, February, 1993.
- [6] L3 Collaboration, O.Adriani *et al.*: Phys. Lett. **B292** (1992) 454.
- [7] L3 Collaboration, O.Adriani *et al.*: Phys. Lett. **B294** (1992) 466.
- [8] J.H.Kühn and P.M.Zerwas: Z Physics at LEP 1, CERN report CERN 89-08, Vol.1, page 267, eds. G.Altarelli *et al.*
- [9] M.Böhm and W.Hollik: Z Physics at LEP 1, CERN report CERN 89-08, Vol.1, page 203, eds. G.Altarelli *et al.*;
S.Jadach and Z.Was: Z Physics at LEP 1, CERN report CERN 89-08, Vol.1, page 235, eds. G.Altarelli *et al.*
- [10] L3 Collaboration, B.Adeva *et al.*: Nucl. Instr. and Meth. **A289** (1990) 35.
- [11] ZFITTER, D.Bardin *et al.*: Z. Phys. **C44** (1989) 493;
D.Bardin *et al.*: Nucl. Phys. **B351** (1991) 1;
D.Bardin *et al.*: CERN-TH.6443/92, May 1992.
- [12] MINUIT, CERN program library, F.James: D506.
- [13] The working group on LEP energy, L.Arnaudon *et al.*: The Energy Calibration of LEP in 1991: preprint CERN-PPE/92-125, CERN, 1992.

- [14] L3 Collaboration, B.Adeva *et al.*: Phys. Lett. **B252** (1990) 713.
T.Aziz: Some interesting approximations of A_{FB} on the Z^0 peak : TIFR-EHEP 90/6, November 1990.
- [15] S.N.Ganguli: On electroweak mixing angle $\sin^2 \theta_{\text{eff}}$ from forward-backward asymmetry of charged lepton and $b\bar{b}$, and τ -polarization: L3-note # 1042, October 1991.

Figure Captions

Figure 1: 68% confidence level contours obtained from a fit to the L3 data in the Standard Model framework: (a) $\sin^2 \bar{\theta}_w$ versus M_Z for Higgs masses of 60 GeV (dotted line), 300–1000 GeV (solid line); (b) $\sin^2 \bar{\theta}_w$ versus M_t for Higgs masses of 60 GeV (dotted line), 300 GeV (solid line) and 1000 GeV (dashed line).

Figure 2: 68% and 95% confidence level contours of $\sin^2 \bar{\theta}_w$ vs \bar{p} obtained from a fit to the L3 data in the model independent approach. The lines indicate Standard Model predictions for various top and Higgs masses. The open circles correspond to top mass values of 100 and 200 GeV.

Figure 3: Values of $\sin^2 \bar{\theta}_w$ from Tables 4 & 5 determined (a) in a model independent fit using leptonic charge asymmetries, b-quark charge asymmetry, tau polarization, and the combined data; (b) within the Standard Model by using Γ_ℓ , Γ_Z , charge asymmetries A_{FB}^ℓ , A_{FB}^b , P_τ , and from a global fit to all data sets. As in Table 4, the upper limits on $\sin^2 \bar{\theta}_w$ from the M_Z plus one of (Γ_ℓ , A_{FB}^b , P_τ) fits are constrained by $\sin^2 \bar{\theta}_w \leq 0.2360$ at $M_H = 300$ GeV.

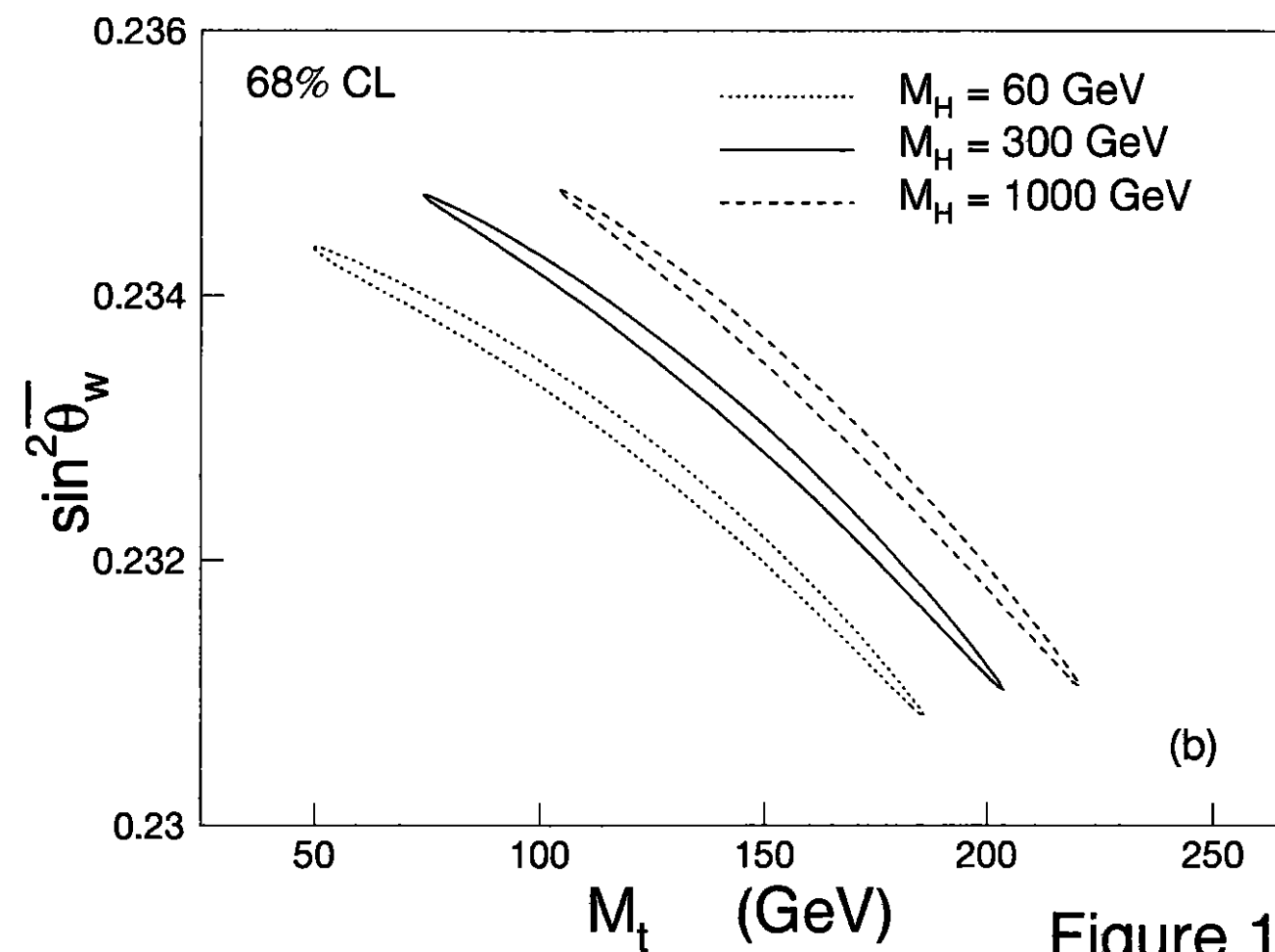
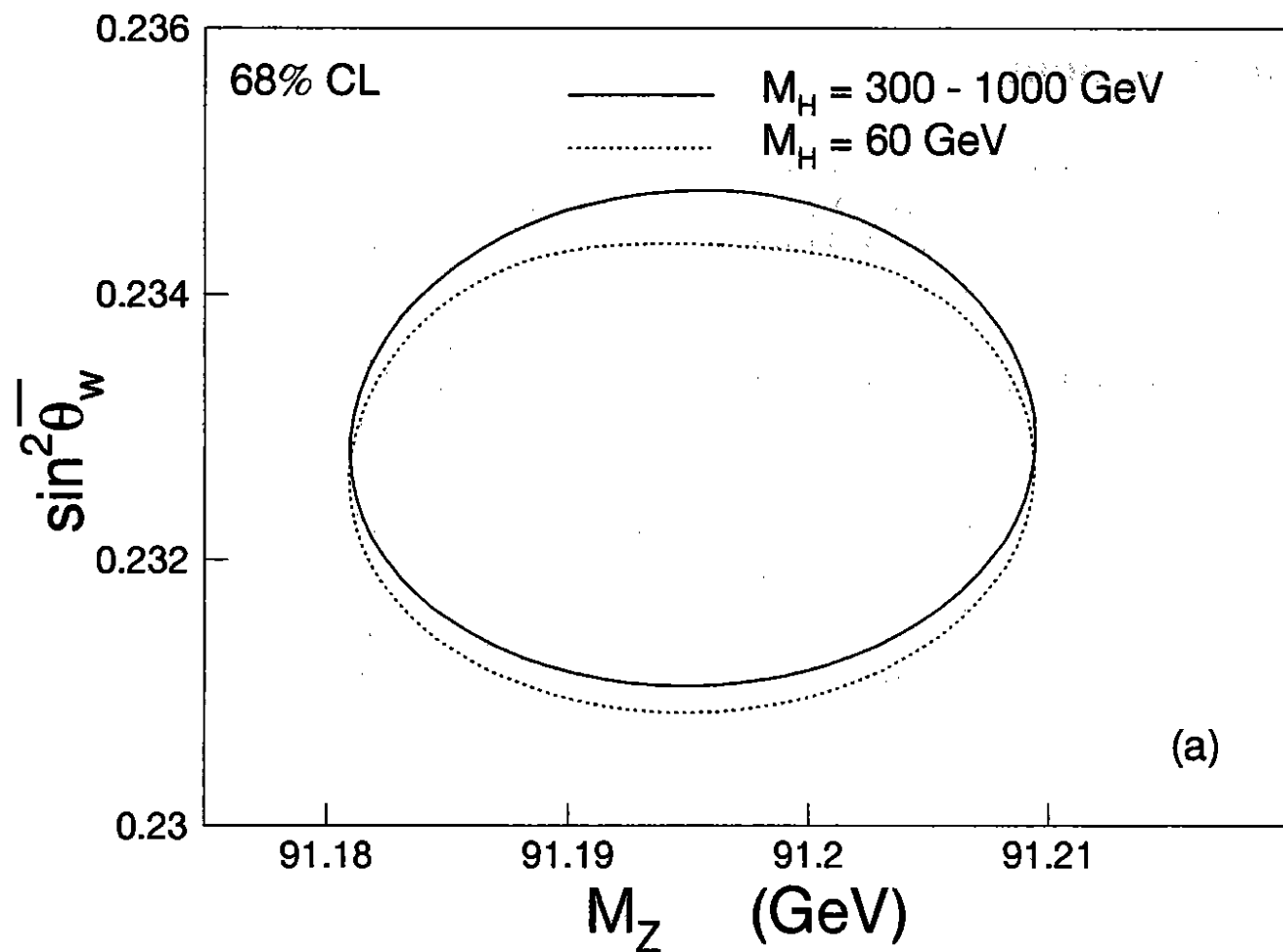


Figure 1

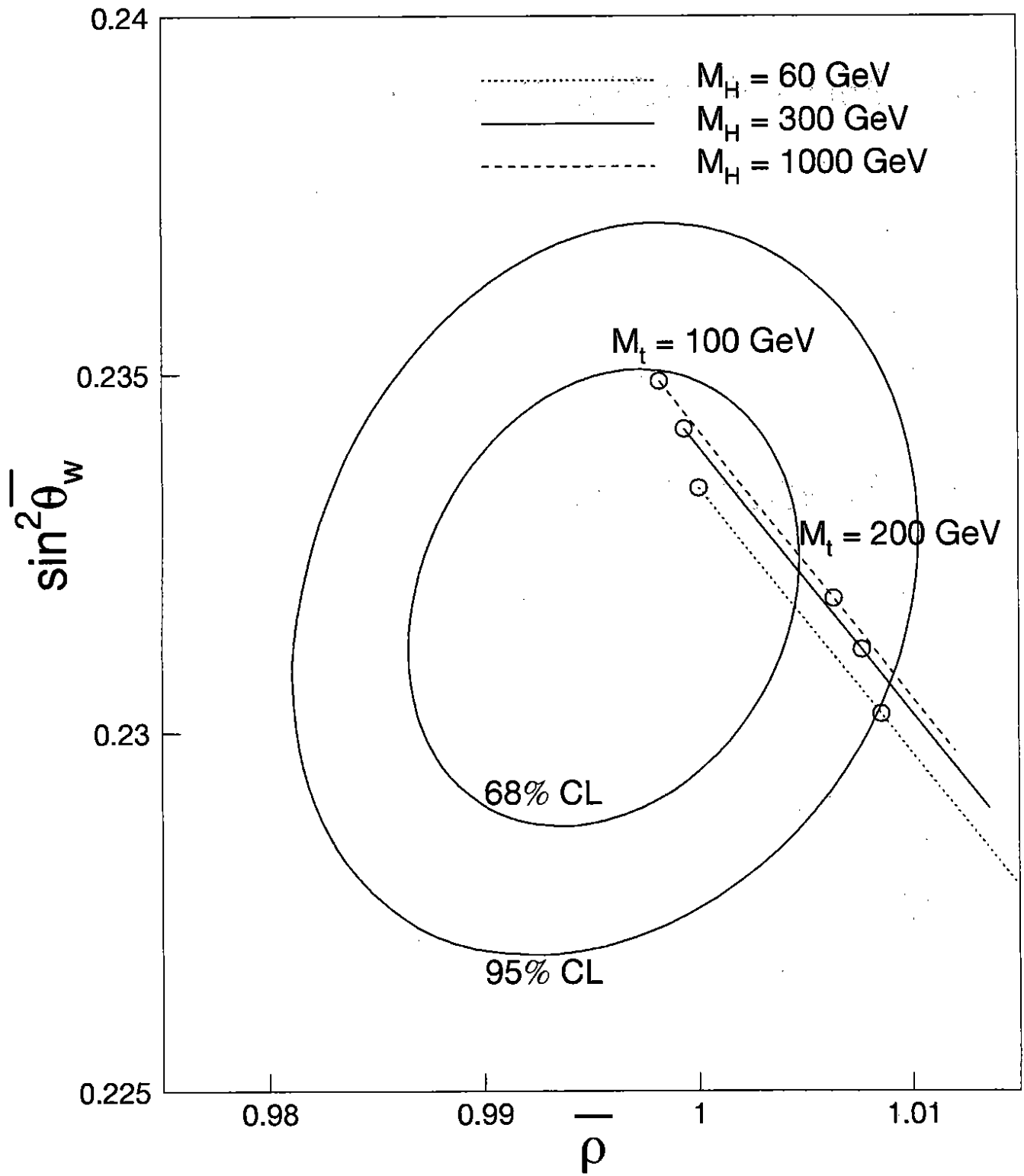


Figure 2

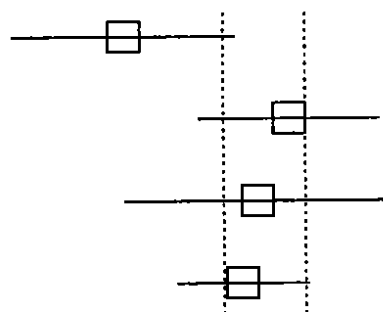
(a) Model Independent

σ 's, A_{FB}^l

σ 's, A_{FB}^b

σ 's, P_τ

σ 's, A_{FB}^l , A_{FB}^b , P_τ



(b) Standard Model

M_Z , A_{FB}^l

M_Z , A_{FB}^b

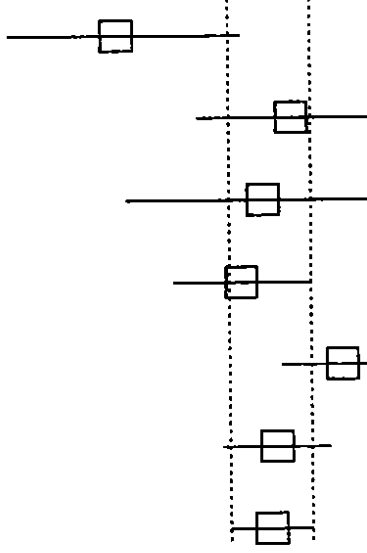
M_Z , P_τ

M_Z , A_{FB}^l , A_{FB}^b , P_τ

M_Z , Γ_l

M_Z , Γ_Z

Global fit



0.21

0.22

0.23

0.24

$\sin^2 \theta_w$

Figure 3